

Classification of retinal blood vessels into arteries and veins using CNN and likelihood propagation

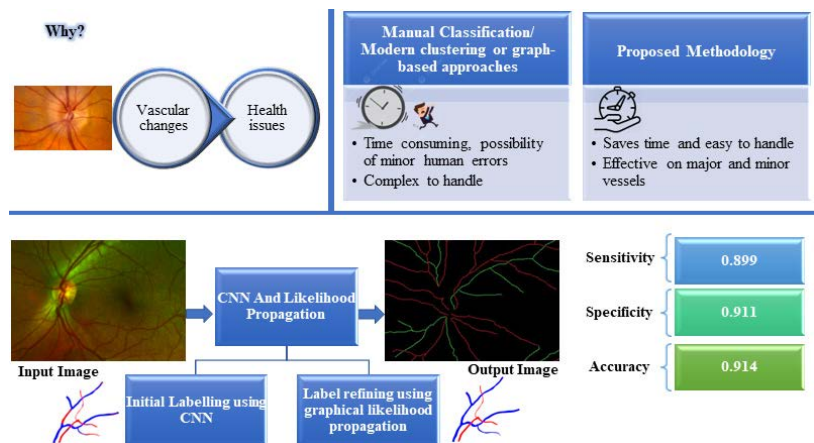
Sarika Patil¹, Yogita Talekar², Swapnil Tathe¹, Sachin Takale³

¹Department of Electronics and Telecommunication Engineering, Sinhgad College of Engineering, Savitribai Phule Pune University, Pune, India. ²Freelance Data Analyst, Pune, India. ³Department of Electronics and Communication Engineering, MIT School of Engineering and Science, MIT Art, Design and Technology University, Pune

Received on: 21-Jun-2024, Accepted and Published on: 11-Sep-2024

ABSTRACT

Retinal Vasculature's altered artery and vein tree structure serves as a clear indicator of many health issues. A critical and required step in the examination and diagnosis of many illnesses is the division of blood vessels into arteries and veins. This work presents a method for classifying arteries and veins in fundus pictures using CNN and likelihood propagation. To improve performance, the suggested strategy combines deep learning and graph analysis techniques. In this procedure, initial labelling is done using CNN, and then the labels are refined using likelihood propagation. The results are compatible with modern clustering or graph-based approaches. The proposed methodology attempts to classify major as well minor vessels and achieves an average value of sensitivity of 0.899 by retaining the value of specificity 0.911 and accuracy 0.914 for VICAR dataset images.



Keywords: Fundus Image; convolutional neural network; likelihood propagation

INTRODUCTION

The eye is a crucial bodily component that aids visualization. Blood vessels, which can be divided into arteries and veins, are part of the anatomy of the human eye. A crucial and important stage in the inspection and diagnosis of many disorders is the classification of blood vessels as arteries and veins.¹ An investigation of the retinal vascular structure, which is connected to a variety of health issues, is made possible by a retinal fundus picture, which immediately depicts vascular anomalies. Since numerous artery-vein-related measurements have been directly linked with the progression of diseases, the research of retinal vascular anomalies in arteries and veins has developed a great deal of interest for retinal image analysis these days.²

The characteristics of the arteries and veins are typically used to classify the body parts. As arteries carry blood with high levels of oxygen to the body's organs while veins carry blood with lower levels of oxygen, veins are darker, and arteries are brighter. Typically, the arteries are thinner than the nearby veins. The central reflex of arteries is wider than that of veins, which have a smaller central reflex. As previously mentioned, the distinction between arteries and veins in the vasculature is crucial for disease diagnosis. One significant sign of diabetes retinopathy, high blood pressure, pancreas, etc. is an abnormal Artery Vein Ratio (AVR). In patients with diabetes, for example, veins are remarkably wide; in patients with pancreatic diseases, arteries are narrower; in patients with high blood pressure, arteries are larger. The regular examination of the retina is necessary to find these illnesses.³

The manual classification of arteries and veins from fundus images and the interpretation of retinal images both involve a lot of work and knowledge. With different cameras being utilized, the resolution and field of vision of the image vary, necessitating very careful viewing.⁴

*Corresponding Author: Sarika Patil, Sinhgad College of Engineering, Pune, India
Email: sarikapatil000@gmail.com

Cite as: J. Integr. Sci. Technol., 2025, 13(1), 1006.

DOI: 10.62110/sciencein.jist.2025.v13.1006

©Authors, ScienceIN <https://pubs.thesciencein.org/jist>

Convolutional Neural Networks (CNNs), a type of neural network where the neurons are locally limited to a certain area of the data, are used in the suggested method. In a variety of biomedical imaging issues, CNNs have produced promising results. In the proposed method, arteries and veins are automatically classified using CNN, and the results of CNN are then propagated using the idea of minimum spanning trees.⁵

RELATED WORK

The proposed vessel classification methods to date can be classified into two broad categories : automatic and semi-automatic. In the case of semi-automatic methods, at first labels are assigned by experts, and subsequently spread throughout the entire network, whereas in case of automatic methods, as the name suggests, categorization forbids any manual contact with the expert. Automated techniques include graph analysis, clustering, machine learning, or a combination of these techniques. A review of these techniques is as mentioned below.

Grisan and Ruggeri⁶ suggested one of the first automatic retinal vascular categorization techniques. A major step in fundus image analysis is vessel network extraction, which is frequently carried out by a vessel tracking procedure and involves the use of a collection of vessel segments. The sparse tracking approach was utilized to automatically extract the vessel network. The retinal image is segmented into a few zones with an equal number of arteries and veins to benefit from local features and vascular network symmetry. It is presumable that the local properties of two different vessel kinds in these zones differ significantly from one another. With this technique, four zones are created around the optic disc, each of which contains one of the primary arches (within 0.5 – 2mm of the optic disc's diameter from its center). Given that this is the first automatic technique, the error was compared to humanly categorized vessels and came out to be 12%; if major boats are considered, the error drops to 7%.

Intensity features are used in techniques by Niemeijer et al.⁷ and Vázquez et al.⁸ to distinguish between veins and arteries. The efficacy of intensity-based Artery/Vein categorization algorithms is directly impacted by the non-uniform illumination and local brightness and contrast variations present in retinal pictures because of the image acquisition procedure.

Marc Saez⁹ suggested a four-step process: first, the vessel profiles were extracted, and then the vascular tree was constructed using a segmentation method. The optimal feature vector was then chosen to differentiate veins from arteries. Ultimately, each discovered vessel was classified as either an artery or a vein using a clustering technique. The outcomes showed that the algorithm is reliable and strong.

The vessel potential connectivity map (VPCM), which consists of vessel segments and the potential connectivity between them, was proposed by Qiao Hu et al.¹⁰. The VPCM is then disambiguated into multiple anatomical trees using a graph-based metaheuristic algorithm. Finally, categorize these trees as artery (A) or venous (V) trees. One of the finest ways to categorize intricate, interconnected retinal veins is by this method.

A graph-based approach was also developed by Behdad Dashtbozorg and Ana Maria Mendonça¹¹, which assigned one of

two labels to each vessel segment and chose the type of each junction point (graph nodes). The final graph-based labelling findings and a set of intensity features are used to classify a vascular segment as either A or V.

To discover the best graph of vessel segments, Joshi et al.¹² graph search method makes use of the orientation, width, and intensity of each vessel segment. Additionally, they exploited the vessels color characteristics in each tree graph. The Arterial-Venous classification of retinal vessels is based on fuzzy C-means clustering, and they have used Dijkstra's technique to identify a vessel subtree.

To lessen the discrepancies in feature space, Xu et al.¹³ utilized a kNN classifier along with intra-image regularization and inter-subject normalization. The DRIVE dataset yields an overall accuracy of 0.923. Vijayakumar¹⁴ employed the Support Vector Machine (SVM) classifier to provide an innovative technique to vessel classification.

A graph cut strategy is also provided by K. Eppenhof et al.¹⁵, which is an expansion of Grisan and Ruggeri⁶ work. It is a brand-new technique for classifying retinal arteries based on local and contextual feature analysis. They have described classification as an optimization issue, as opposed to earlier graph-based approaches, based on a non-submodular energy function that is precisely and effectively minimized using the Quadratic Pseudo-Boolean Optimization (QPBO) graph cut algorithm.

According to F. Huang et al.¹⁶ proposed, the method that uses only centerline pixel information performs well than the method that uses complex graph analysis. The graph analysis of the retinal blood vessels shows connectivity of the vessels with pixel-wise classification.

Like Pellegrini¹⁷ proposed method, graph cut approach is used to compute a globally optimal separation between the arterial and venular networks from a graph representation created using hand-crafted features based on local vessel intensity and vascular morphology. However, they employed a UWFoV SLO Local Database, a scanning laser ophthalmoscope with an ultra-wide field of view that is less common in ordinary opticians than fundus cameras.

Hu et al.¹⁸ Vessel-constrained network for autonomous AV classification uses a CNN model based on the U-net.

The MSGANet-RAV¹⁹ technique provides a multiscale attention network for pixelwise AV classification. Because it combines multiscale feature extraction with a succession of GF and context-learnable SVA modules, this method is difficult to put into practice.

A novel Multi-task Segmentation and Classification Network (MSC-Net) was proposed by Junyan Yi et. al.²⁰. It introduces three modules to improve the performance of A/V classification: a Multi-scale Vessel Extraction (MVE) module that uses the semantics of vessels to distinguish between vessel pixels and background; a Multi-structure A/V Extraction (MAE) module that classifies arteries and veins by combining the original image with the vessel features produced by the MVE module; and a Multi-source Feature Integration (MFI) module that combines the outputs of the previous two modules to obtain the final A/V classification results. On numerous public datasets, extensive empirical trials confirm the

superior performance of the suggested MSC-Net for retinal A/V classification compared to cutting-edge techniques.

An innovative technique based on generative adversarial networks with enhanced U-Net is put forth by Jieni Zhang et. al.²¹ and can accomplish synchronous automatic segmentation and classification of blood vessels via an end-to-end network. By using the suggested approach, the segmentation results from several classification tasks are not dependent on one another. Furthermore, the suggested approach classifies arteriovenous crossings in addition to accurately categorizing arteries and veins. The RITE dataset is used to assess the validity of the suggested method; the accuracy of picture comprehensive classification is 96.87%. Arteriovenous categorization has a sensitivity and specificity of 91.78% and 97.25%, respectively. The outcomes demonstrate the competitive classification performance and validate the efficacy of the suggested approach.

The reviewed literature mentions that numerous problems with the artery vein classification were discovered throughout the research of the literature. These limitations are stated below:

- The absolute hue of blood in veins varies between photos and even within the same subject poses a significant classification challenge. The degree of hemoglobin oxygen saturation, aging and cataract development, variations in flash intensity and spectrum, nonlinear optical distortions of camera, flash artifacts and focus are a few causes of variability.
- There are differences due to cataracts, macular edema, hemorrhages and tortuosity brought on by different illnesses.
- Other crucial element to be considered is image resolution.
- In addition to being variable along the vessel, vessel thickness is significantly impacted by vessel segmentation, making it an unreliable trait for categorization.

All these factors have an impact on the system's accuracy, which makes the autonomous categorization of veins and arteries a very difficult computational task. The constraints indicated above led us to employ an AV classification technique based on CNN and probability, which attempts to overcome many shortcomings.

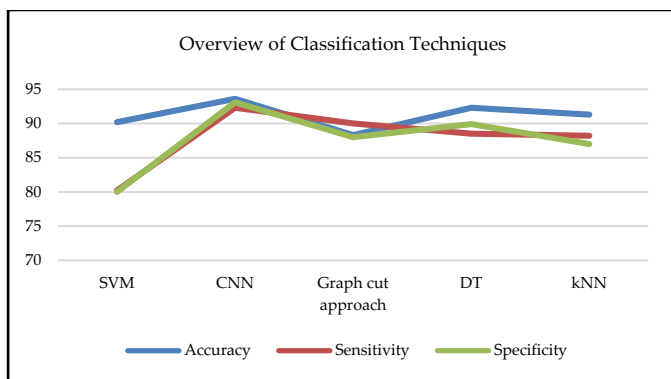


Figure 1. Overview of Artery/Vein Classification Techniques.

Figure 1 illustrates comparison of some of the previously proposed classification methods and clearly shows that CNN-based categorization offers the best metrics in terms of accuracy, sensitivity, and specificity.

MATERIAL

A. Database Used

The proposed approach of AV classification was tested on the openly available dataset VICA VR. A collection of retinal images from the VICA VR database is utilized to calculate the Arteriovenous ratio. This collection contains 58 images with a resolution of 768 × 584 pixels, captured using a Topcon nonmydriatic camera type NW-100. The database also contains the vessel type (artery/vein) assigned by three specialists as well as the caliber of the vessels measured at various distances from the optic disc. Database was taken from <http://www.varpa.es/research/ophtalmology.html#vicavr>.

B. Performance Measures

The three most crucial performance metrics for the classification of retinal blood vessels are accuracy, sensitivity/True Positive rate (TPR), and specificity as described in Table 1. Four possible categorization scenarios include the division of retinal blood vessels into arteries and veins, based on two accurate and two inaccurate classifications. The true positive (TP) condition occurs when the model correctly identifies an instance as an artery when it actually is an artery. True negative (TN) the model correctly identifies an instance as a vein when it actually is a vein. The two errors are the false positive (FP), the model incorrectly identifies an instance as an artery when it actually is a vein, and the false positive (FP), the model incorrectly identifies an instance as a vein when it actually is an artery.

Table 1. Performance Measures

Performance Measures	Formulae
Accuracy	$(TP+TN)/(TP+FP+TN+FN)$
Sensitivity/TPR	$TP/(TP+FN)$
Specificity	$TN/(TN+FP)$

METHODS

The initial classification using CNN and its propagation to the output in the vasculature are the first two steps of the proposed classification technique. The second step, known as probability propagation, entails CNN labelling that will be transmitted to the vascular network. The CNN does segmentation first, followed by classification. The proposed method's block diagram is shown in Figure 2.

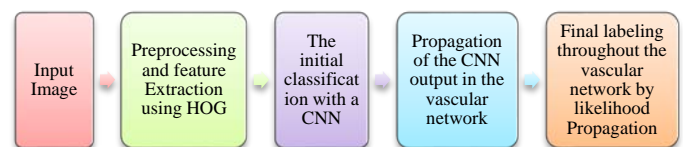


Figure 2. Block Diagram of Proposed Method

Preprocessing and feature Extraction

The RGB input image is simplified by being made grayscale, and it is then enlarged, which will simplify computations for subsequent operations. To bring out the features of the scaled image, the top-hat filter is used. The top-hat filter, also known as white top-hat filter, is typically used to highlight bright subjects against a dark

background. To emphasize dark objects of interest against a bright background, the black-hat operation (bottom-hat filter or black top-hat filter) is used. The top-hat filter is used to adjust uneven lighting. According to the size of structuring element, filters essentially keeps small regions and suppress the larger ones. This is employed solely for aesthetic reasons. Here, a 10 pixel radius disk-shaped structural element has been used. The top-hat filtered image is then combined with the scaled RGB image to create an improved image.

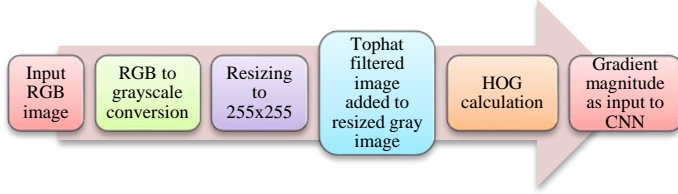


Figure 3. Preprocessing and feature Extraction

The HOG (histogram-oriented gradients) algorithm is then applied to this image. Object detection frequently makes use of the HOG features. A picture is divided into tiny, squared cells using HOG, which then computes a histogram of oriented gradients in each cell, normalizes the outcome using a block-wise pattern, and outputs a descriptor for each cell. An object detection classifier such as SVM uses the stacking of cells into a squared image region as an image window descriptor. The gradient magnitude is employed as the CNN classifier’s input in the proposed model. The utilized feature extraction and preprocessing stages are shown in Figure 3.

B. Training strategy of CNN

A region of an image measuring $n \times n$ pixels is downsized to $28 \times 28 \times 1$ for input into the top layer. Each convolutional layer i at depth n , represented as l_i^n , calculates a local 9×9 convolution from the input patch or the output of the preceding layer, adds a bias, and then produces the output by using a rectified linear unit (ReLU) as specified in Equation 1. Figure 4 illustrates the proposed CNN model with seven layers.

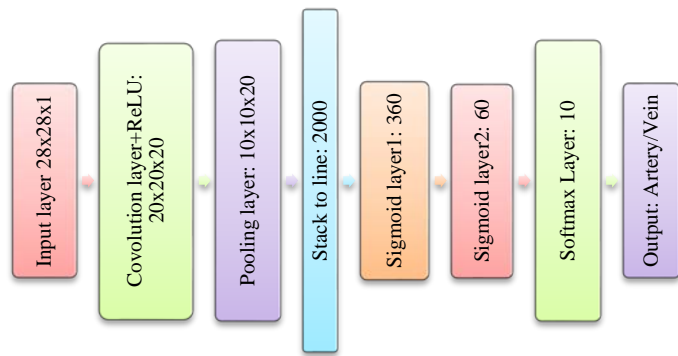


Figure 4. Proposed CNN Model

The trainable parameters for every 2D convolution are the biases b_i^n and the weights w_{nm}^i .

$$l_n^i = \text{Avg} (0, \sum_m l_n^{i-1} * w_{nm}^i + b_n^i) \tag{1}$$

Here the parameters like kernel weights w_{nm}^i and bias b_n^i are the trainable parameters. Since a max pooling layer follows every convolutional layer, reducing the feature map’s size by 2, the max is computed on a 2×2 kernel. The vector is finally resolved into one of the two classes (artery or vein) by a SoftMax classifier based on the produced probability values.

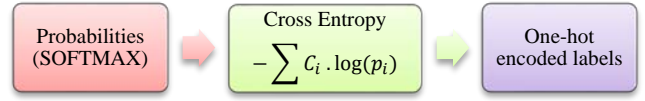


Figure 5. Cross Entropy Reference

Softmax function normalises results on a [0, 1] scale. In softmax the sum of outputs will always be equal to 1. Afterwards, binary outputs are transformed by using one hot encoding. As a result, the neural network’s output layer receives one hot encoding and a softmax, respectively. The projected categorization output would then be real labelled output. In this case, probabilities and one hot encoded labels are correlated using the cross entropy function. Figure 5 displays the Cross Entropy reference idea.

The cross-entropy loss function is given by,

$$E = -\frac{1}{N} (\sum_{i=1}^N c_i \cdot \log(p_i)) \tag{2}$$

Where c refers to one hot encoded class whereas p refers to SoftMax applied probabilities. The base of \log is e .

Note that the probability and scores from neural network are calculated first before applying SoftMax. After applying cross entropy to the SoftMax applied probability, one hot encoded class is generated. It is necessary to ascertain the derivative of total error with respect to one another as a result. The Backward Error Calculation via Chain Rule concept is depicted in Figure 6.

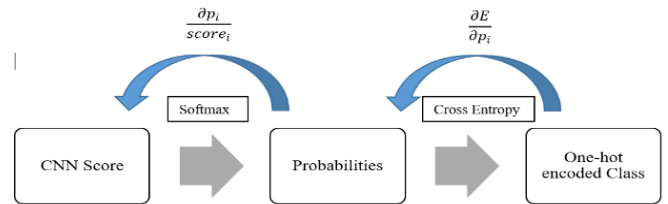


Figure 6. Backward Error Calculation by Chain rule

Here are the backward error calculation's equations:

$$\frac{\partial E}{\partial score_i} = \left(\frac{\partial E}{\partial p_i} \right) \cdot \left(\frac{\partial p_i}{\partial score_i} \right) \tag{3}$$

$$\frac{\partial E}{\partial p_i} = \frac{-c_i}{p_i} + \frac{1-c_i}{1-p_i} \tag{4}$$

$$\frac{\partial p_i}{\partial score_i} = p_i \cdot (1 - p_i) \tag{5}$$

Thus, putting equation 4 & 5 in equation 3 we will get,

$$\frac{\partial E}{\partial score_i} = p_i - c_i \tag{6}$$

C. Likelihood Propagation

The result of CNN classification at position (x, y) is a score $S(x, y)$, which indicates how likely an artery or vein is based on the

score of 1 or 0. As CNN only has a limited understanding of the tree structure, CNN's output labelling is improved through likelihood propagation. The vessel branch score is created by averaging the likelihood scores for each pixel, and the branch score is then communicated to the network using graph representation.

Vessel Branch Extraction:

The segmented vessel's skeleton is first obtained, and then the crossings and bifurcations are examined to produce the connected nodes of the vessel tree. The connected components are found for each branch b_i , and the endpoints, x_1^i and x_2^i , with the orientation, α_1^i and α_2^i , are noted.

Representation of graph:

Vessel tree is represented as unidirectional graph $G = (V, E)$ with the cost function $c = E \rightarrow R$. This graph's nodes each represent a vessel branch b_i . The branch's potential of being an artery is related to the node, S_i . The labels $s(x; y)$ taken from the CNN classification and recentered around 0 in Equation 7 are used to obtain this score.

$$s_i = s(b_i) = \frac{1}{N_i} \sum_{x,y \in b_i} s(x, y) - 0.5 \quad (7)$$

The possibility that two network nodes (i.e., vessel branches) will be joined is likewise correlated with the cost. This cost is created through the addition of the location cost by the labelling cost, abbreviated as c_{pos} and c_{lab} . To favor the connection of collinear branches, the position component is calculated using the minimal distance between each branch's two end points, with an additional cost of λ_{angle} on angles. The score difference between the two branches is used by the label component.

$$c_{pos}(b_i, b_j) = \frac{1}{\sigma_{pos}} \min_{k \in \{1,2\}, l \in \{1,2\}} |x_k^i - x_l^j| + \lambda_{angle} |\alpha_1^i - \alpha_2^j| \quad (8)$$

$$c_{lab}(b_i, b_j) = \frac{1}{\sigma_{lab}} |s_i - s_j| \quad (9)$$

The influence of the position cost in relation to the label cost is controlled by the parameters σ_{pos} and σ_{lab} .

D. Minimum spanning tree and propagation of score:

The algorithm of minimum spanning tree is used to simplify the graph. In this tree, every node receives a likelihood score from another node indicating whether it is more likely to be an artery or vein. This likelihood value is then attenuated by the total location cost between the two nodes. First, a post-order path through the tree from child to parent is taken with the likelihood scores from each node. A position cost called $c_{pos}(b_i, P(b_i))$ is added to the parent's current score to attenuate each child's score before it is sent.

$$s_i^\uparrow = s^\uparrow(b_i) = s_i + \sum_{P(b_j)=b_i} \exp\left(\frac{c_{pos}(b_i, b_j)}{\sigma_{prop}}\right) s_j^\uparrow \quad (10)$$

Each parent then sends the likelihood score s_i^\uparrow to each of its children, which now incorporates the total score from all subtrees, minus the likelihood score that child has previously provided, to get the final score s_i^{fin} .

$$s_i^{fin} = s_i + \exp\left(\frac{c_{pos}(b_i, P(b_i))}{\sigma_{prop}}\right) [s^{fin}(P(b_i)) - \exp\left(\frac{c_{pos}(b_i, P(b_i))}{\sigma_{prop}}\right) s_i^\uparrow] \quad (11)$$

The labels are improved in accordance with the final score, and σ_{prop} controls the attenuation cost. If the result is negative or positive, the object is categorized as an artery or a vein, respectively.

EXPERIMENTAL RESULTS

The publicly accessible VICA VR database having 58 images with a resolution of 768 x 584 is used to evaluate the proposed classification methodology. The CNN training method uses the Signal and Label files.

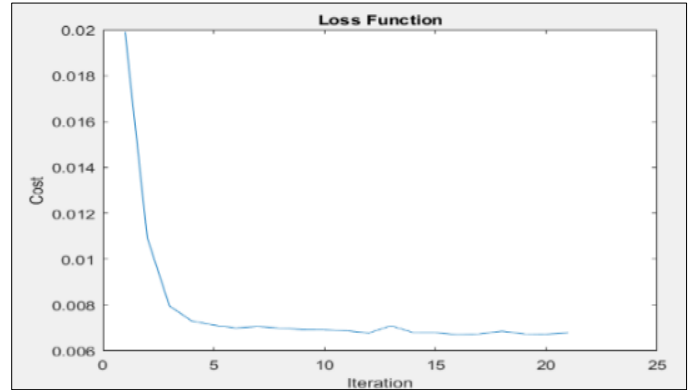


Figure 7. Plot of Loss function during Training

The initialization of the trainable parameters is random. The forward propagation is performed using these random values, and the cross-entropy function as defined by Eq. 2 is used to determine the cost. Iteratively travelling in the direction of the steepest fall, as indicated by the negative of the gradient, gradient descent is an optimization process used to minimize some function. In the suggested approach, stochastic gradient descent is used to minimize the cross-entropy loss function as the weights and biases evolve for each batch size of n batch, loss function is as plotted in Figure 7.

We employ data augmentation during the training phase, which entails adding random changes to the training samples, to prevent overfitting the model. Particularly in the case of medical imaging, the transformations used must be realistic given the nature of the input data. We apply random rotations to every patch as a geometric enhancement. Likelihood propagation enhances CNN's output labeling since CNN's comprehension of the tree structure is restricted. The probability scores for each pixel are averaged to form the vessel branch score, which is then provided to the network via graph representation.

The performance metrics i.e. sensitivity, specificity and accuracy used for evaluation are as defined in Table 1. Figure 8 displays the results of the suggested technique where veins are indicated with green color in Figure 8(e) whereas the segmentation of arteries and veins are as shown in Figure 8 (c and d) respectively.

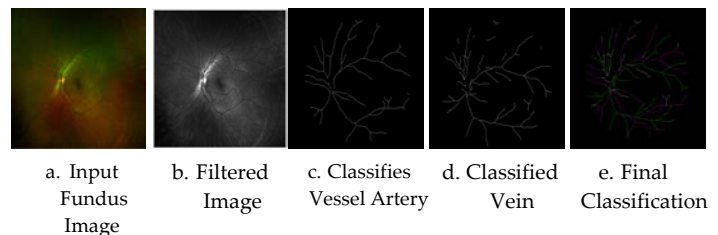


Figure 8 Results: Artery Vein Segmentation and Classification

The evaluation metrics that are acquired through pixel-by-pixel measurement are contrasted with the most advanced techniques. It is discovered that the suggested algorithm, in contrast to other literature approaches, concentrates on and strikes a balance between rejecting the false pixels in the segmented results and detecting the true ones. It is important to note that the evaluation metrics are compatible with the other state of the art methods as shown in Table 2.

Table 2. comparison of results for a/v classification based on evaluation parameters with state-of-art methods

Methods	Database	Sensitivity	Specificity	Accuracy
Pellegrini et al. ¹⁷	WIDE	-	-	0.883
Hu et al. ¹⁸	DRIVE	0.936	0.974	0.955
F.Sohel et al. ¹⁹	DRIVE	0.935	0.972	0.954
Chen et.al. ²⁰	DRIVE	0.9494	0.9441	0.9469
	LES	0.9030	0.9155	0.9072
Zhang et. al. ²¹	RITE	0.9178	0.9725	0.9687
Estrada et al. ²²	WIDE	0.910	0.909	0.910
J Morano et al. ²³	RITE	0.874	0.908	0.892
Girard et al. ²⁴	DRIVE	0.863	0.866	0.865
Proposed Method	VICAVR	0.899	0.911	0.914

DISCUSSIONS

An attempt is made to compare the performance of the suggested approach with both conventional and state-of-the-art methods for A/V categorization, as indicated in table no 2. The datasets utilized for testing are distinct with varying resolutions, even if the comparison is displayed with evaluation characteristics like sensitivity, specificity, and accuracy. The authors discovered that there were fewer experiments on VICAR for A/V categorization. However, the suggested approach is found to be compatible with the other methods listed in Table No. 2 with respect to the specified parameter values. The proposed approach uses individual pixels to classify veins and arteries.

When compared to cascades of real CNNs, the use of HOG feature extraction has improved CNN feature extraction and functioned as a CNN cascade with less training parameters. Better interpretation of the output pixels was achieved by using likelihood propagation at the CNN's output.

For the two-class classification problem (artery or vein), our CNN architecture uses a softmax output layer; however, a sigmoid function might also be used in this situation. For binary classification jobs such as ours, a sigmoid function would be a more conventional choice, since softmax is usually applied to multi-class issues. However, softmax was chosen in our implementation due to the limitations of current architecture. Investigating the usage of sigmoid functions in CNNs for binary classification in future research may yield an intriguing comparison.

CONCLUSIONS

The proposed method is a fusion of CNN and likelihood score propagation. CNN is used for initial labeling and the labels are refined using likelihood propagation. As this method combines the two techniques, the performance of this method is better than the state-of-the-art methods. Due to the small field of view (FOV) in

normal fundus imaging, occlusions are more common than in this approach, making it more reliable. By using global propagation in the subtrees where parts of the network are disconnected, our strategy surpasses earlier work on public databases. Although some of the performance measures of previously used methods in table shows higher numbers, the methods are complex to implement as compared with proposed method.

By using multi-modal fusion techniques to combine supporting data from other scanning modalities, like as fluorescein angiography and OCT, a more comprehensive view of the retinal vasculature and the course of the illness can be provided.

CONFLICT OF INTEREST

The authors declare that they do not have any conflict of interest.

REFERENCES

1. Y. Yang, S. Huang, N. Rao. An Automatic Hybrid Method for Retinal Blood Vessel Extraction. *Int. J. Appl. Math. Comput. Sci.* **2008**, 18 (3), 399–407.
2. Q. Mirsharif, F. Tajeripour, H. Pourreza. Automated characterization of blood vessels as arteries and veins in retinal images. *Comput. Med. Imaging Graph.* **2013**, 37 (7–8), 607–617.
3. C. Muramatsu, Y. Hatanaka, T. Iwase, T. Hara, H. Fujita. Automated selection of major arteries and veins for measurement of arteriolar-to-venular diameter ratio on retinal fundus images. *Comput. Med. Imaging Graph.* **2011**, 35 (6), 472–480.
4. Q. Chen, J. Peng, S. Zhao, W. Liu. Automatic artery/vein classification methods for retinal blood vessel: A review. *Comput. Med. Imaging Graph.* **2024**, 113 (2), 102355.
5. F. Girard, C. Kavalec, F. Chriet. Joint segmentation and classification of retinal arteries/veins from fundus images. *Artif. Intell. Med.* **2019**, 94, 96–109.
6. E. Grisan, A. Ruggeri. A divide et impera strategy for automatic classification of retinal vessels into arteries and veins. In *Annual International Conference of the IEEE Engineering in Medicine and Biology - Proceedings*; **2003**; Vol. 1, pp 890–893.
7. M. Niemeijer, X. Xu, A. V. Dumitrescu, et al. Automated measurement of the arteriolar-to-venular width ratio in digital color fundus photographs. *IEEE Trans. Med. Imaging* **2011**, 30 (11), 1941–1950.
8. S.G. Vázquez, B. Cancela, N. Barreira, et al. Improving retinal artery and vein classification by means of a minimal path approach. *Mach. Vis. Appl.* **2013**, 24 (5), 919–930.
9. M. Saez, S. González-Vázquez, M. González-Penedo, et al. Development of an automated system to classify retinal vessels into arteries and veins. *Comput. Methods Programs Biomed.* **2012**, 108 (1), 367–376.
10. Q. Hu, M.D. Abramoff, M.K. Garvin. Automated construction of arterial and venous trees in retinal images. *J. Med. Imaging* **2015**, 2 (4), 044001.
11. B. Dashtbozorg, A.M. Mendonca, A. Campilho. An automatic graph-based approach for artery/Vein classification in retinal images. *IEEE Trans. Image Process.* **2014**, 23 (3), 1073–1083.
12. V.S. Joshi, J.M. Reinhardt, M.K. Garvin, M.D. Abramoff. Automated method for identification and artery-venous classification of vessel trees in retinal vessel networks. *PLoS One* **2014**, 9 (2), 2.
13. X. Xu, W. Ding, M.D. Abramoff, R. Cao. An improved arteriovenous classification method for the early diagnostics of various diseases in retinal image. *Comput. Methods Programs Biomed.* **2017**, 141, 3–9.
14. V. Vijayakumar, D.D. Koozekanani, R. White, et al. Artery/vein classification of retinal blood vessels using feature selection. In *Proceedings of the Annual International Conference of the IEEE Engineering in Medicine and Biology Society, EMBS*; **2016**; Vol. 2016-October, pp 1320–1323.
15. K. Eppenhof, E. Bekkers, T.T.J.M. Berendschot, J.P.W. Pluim, B.M. ter Haar Romeny. Retinal Artery/Vein Classification via Graph Cut Optimization. In *Proceedings of the Ophthalmic Medical Image Analysis Second International Workshop, OMA*; **2017**; pp 121–128.

16. F. Huang, B. Dashtbozorg, T. Tan, B.M. ter Haar Romeny. Retinal artery/vein classification using genetic-search feature selection. *Comput. Methods Programs Biomed.* **2018**, 161, 197–207.
17. E. Pellegrini, G. Robertson, T. Macgillivray, et al. A Graph Cut Approach to Artery/Vein Classification in Ultra-Widefield Scanning Laser Ophthalmoscopy. *IEEE Trans. Med. Imaging* **2018**, 37 (2), 516–526.
18. J. Hu, H. Wang, Z. Cao, et al. Automatic Artery/Vein Classification Using a Vessel-Constraint Network for Multicenter Fundus Images. *Front. Cell Dev. Biol.* **2021**, 9, 9.
19. A.Z.M.E. Chowdhury, G. Mann, W.H. Morgan, et al. MSGANet-RAV: A multiscale guided attention network for artery-vein segmentation and classification from optic disc and retinal images. *J. Optom.* **2022**, 15, S58–S69.
20. J. Yi, C. Chen. Multi-Task Segmentation and Classification Network for Artery/Vein Classification in Retina Fundus. *Entropy* **2023**, 25 (8), 8.
21. J. Zhang, K. Yang, Z. Shen, et al. End-to-End Automatic Classification of Retinal Vessel Based on Generative Adversarial Networks with Improved U-Net. *Diagnostics* **2023**, 13 (6), 6.
22. R. Estrada, M.J. Allingham, P.S. Mettu, et al. Retinal Artery-Vein Classification via Topology Estimation. *IEEE Trans. Med. Imaging* **2015**, 34 (12), 2518–2534.
23. J. Morano, Á.S. Hervella, J. Novo, J. Rouco. Simultaneous segmentation and classification of the retinal arteries and veins from color fundus images. *Artif. Intell. Med.* **2021**, 118, 102–116.
24. F. Girard, C. Kavalec, F. Chriet. Joint segmentation and classification of retinal arteries/veins from fundus images. *Artif. Intell. Med.* **2019**, 94, 96–109.